Communication

Electromagnetic Effective-Degree-of-Freedom Prediction With Parabolic Equation Method

Yinsong Shen, Zi He, Wei E. I. Sha, Shuai S. A. Yuan, and Xiaoming Chen

***Abstract*— The performance of a multiple-input-multiple-output (MIMO) wireless communication system can usually be indicated by its effective degree of freedom (EDOF). The parabolic equation (PE) method is widely used to predict electromagnetic (EM) propagation loss for its simplicity and efficiency. A novel PE-based EM channel model is first established for acquiring the EDOF in an electrically large and complex environment. At first, the accuracy of the proposed PE Model is verified by comparing it with the dyadic Green's function. It is shown that the PE Model produces the same results as the analytical one. Then, the connection between the limit of the EM EDOF and the optimal source/receiver numbers is analyzed in the inhomogeneous environment with obstacles. Finally, a complex urban environment is analyzed and the sensitivity analysis is made for the EM EDOF. Numerical results show that the EM EDOF will be stable when the number of transmitting/receiving array sources reaches a certain point. The proposed PE model can be used as an efficient tool for evaluating communication channels in complex environments.**

***Index Terms*— Complex environment, EM effective degrees of freedom (EDOF), MIMO wireless communications, parabolic algorithm.**

I. Introduction

In practical multiple-input-multiple-output (MIMO) wireless communications, the performances of communication channels are affected by many factors, such as the number of antennas, transmitting power, and specific propagating environments. Based on Shannon's information theory [1], MIMO technology has increased the capacity and reliability of the communication system [2]. According to information theory, the EDOF is defined to characterize the performance of communication systems.

Generally, the EDOF can be calculated with the singular values of the channel matrix [3]. The channel matrix is usually modeled based on the far-field approximation in free space [4], or some approximation methods tailored to the multipath environment [3], while these models cannot capture the full-wave physical information of EM fields. Based on the dyadic Green's function, the free space electromagnetic (EM) channel matrix is built for investigating near-field communication [5]. However, the actual radio wave propagation environment is complicated, involving mountainous areas and cities. The wireless communication signals will be greatly affected by physical obstacles. As a result, the transmission performance of the communication system will be significantly modified. Therefore, it is necessary to consider the impact of a complex environment for establishing a high-performance base station configuration.

In the past decades, many propagation models have been proposed to analyze radio wave propagation in complex environments.

However, due to a large amount of calculation in complex environments, the wireless propagation prediction of the traditional models is extremely complicated. In the past years, the parabolic equation (PE) method has made great achievements in the fields of EM wave propagation and EM scattering. The implicit finite difference method of the Crank–Nicolson (CN) scheme has been traditionally used to solve the PE method [6], [7], [8], [9], [10]. However, the CN scheme becomes computationally intensive when dealing with dense meshes. Then the ADI-PE method was proposed to reduce the amount of calculation [11], [12], [13]. Later, based on the ADI-PE method, some schemes were proposed to further reduce both the CPU time and the memory requirement [14], [15]. Although the FD method is widely used to solve PE with low complexity, the computational accuracy becomes worse as the electrical size increases especially for long-range propagation problems. Therefore, for the EM propagation problems, the split-step Fourier transforms (SSFT)-based PE method is widely used to analyze irregular terrain [16], [17], [18], [19], [20], tunnels [21], [22], [23], [24], tropospheric propagation [25], and sea surface [26]. In recent years, PE has been used to analyze the diffraction and other problems of the urban environment [27], [28], [29]. The traditional SSFT is solved by the odd-even decomposition method, which will increase the calculation time. After that, the SSFT algorithm based on the alternating-direction-decomposition method (ADD-SSFT) was proposed. This scheme has simplified the SSFT algorithm by decomposing the diffraction term into three terms. It reduces the two-dimensional Fourier transform to a one-dimensional Fourier transform, which greatly improves the efficiency of the solution. Moreover, the boundary could be accounted for both for the integer and half lattice [30].

In this communication, a PE model is established for the sensitivity analysis of the EDOF in a complex environment. The ADD-SSFT scheme is used to solve the PE. First, compared with the analytical method, the accuracy of the proposed PE model is verified. Second, the connection between the limit of the EM EDOF and the optimal source/receiver numbers is analyzed in the inhomogeneous EM environment with obstacles. At last, the complex urban environment is modeled and the sensitivity of the EDOF is analyzed. The numerical PE method proposed can be used to establish the channel model of wireless communications.

II. Theory and Implementation

A. Scalar EM Channel Model Based on the ADD-SSFT PE Method

As shown in Fig. 1, a set of N_T transmitting antennas is distributed on the transmitter plane and N_R receiving antennas are distributed on the receiver plane. In order to get antenna de-embedded channels, the transmitting and receiving antennas are modeled as isotropic

Manuscript received 24 August 2022; revised 17 November 2022; accepted 27 December 2022. Date of publication 9 January 2023; date of current version 7 April 2023. This work was supported in part by the Natural Science under Grant 62071231, Grant 61890541, and Grant 61931021; in part by Jiangsu Province Natural Science Foundation under Grant BK20211571; and in part by the Fundamental Research Funds for the Central Universities under Grant 30921011207. *(Corresponding author: Zi He.)*

Yinsong Shen and Zi He are with the School of Electrical Engineering and Optical Technique, Nanjing University of Science and Technology, Nanjing 210094, China (e-mail: sys@njust.edu.cn; zihe@njust.edu.cn).

Wei E. I. Sha and Shuai S. A. Yuan are with the College of Information Science and Electronic Engineering, Zhejiang University, Hangzhou 310027, China.

Xiaoming Chen is with the School of Information and Communications Engineering, Xi'an Jiaotong University, Xi'an 710049, China.

Color versions of one or more figures in this communication are available at https://doi.org/10.1109/TAP.2022.3233487.

Digital Object Identifier 10.1109/TAP.2022.3233487

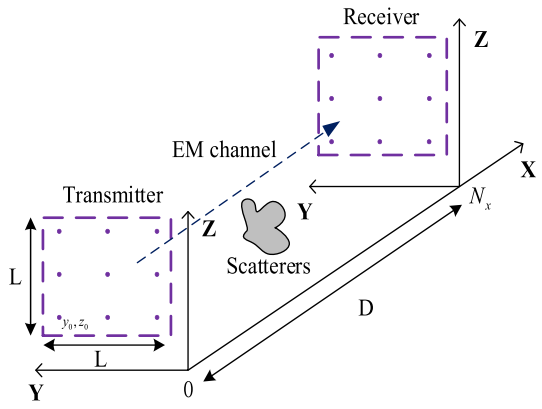

Fig. 1. EM channel model based on the ADD-SSFT PE method. A communication system consists of $N_T = N_R$ uniformly distributed point source transmitters/receivers on the transmit/receive plane. D is the distance between the transmitter and receiver planes, and L is the side length of the planes. $N_x = D/\Delta x$, $N_y = L/\Delta y$, and $N_z = L/\Delta z$ represent the number of discretions along the x, y, and z directions, respectively.

point sources/receivers, which is a widely used approach for the DOF/EDOF analysis [5], [31]. From an EM perspective, the antennas can also be modeled as continuous surface (equivalent) currents by rooftop or Rao–Wilton–Glisson (RWG) basis, as frequently utilized in the methods of moments. Different basis representations of the currents, which relate to different antenna designs, will not influence the estimations of the EDOF and DOF limit. In other words, it is independent of the current distribution. Actually, it depends on the operator properties of Green's function. It is worth noting that the EDOF will be slightly increased by the coupling between antenna elements, but the variation trend of EDOF will not be changed. And the antennas commonly used in MIMO are larger than half wavelength so that the coupling between the antennas can be ignored [32], [33], [34]. Therefore, the point sources can be regarded as half-wavelength antennas, and the mutual coupling between antenna elements is ignored here to draw a fundamental physical conclusion and explore insightful engineering rules.

The SSFT solution of the three-dimensional PE in free space can be written as

$$u\left(x+\Delta x, y, z\right) = \mathrm{e}^{[ik\Delta x(n-1)]} \cdot \Im^{-1}\left[\mathrm{e}^{(ik_x\Delta x)}\Im\left[u(x, y, z)\right]\right] \quad (1)$$

where $\Im^{-1}$is the IFFT and $\Im$ represents the FFT, $\mathrm{e}^{(ik_x\Delta x)} = \mathrm{e}^{(i\Delta x(k^2 - k_y^2 - k_z^2)^{1/2})}$ is the diffraction term.

It can be seen from (1) that the diffraction term in the angular spectral domain is composed of wavenumber in both directions. In order to reduce the dimension of the step calculation process of the PE method, the diffraction factor can be decomposed into two irrelevant diffraction terms and one phase term

$$K(k_y, k_z) \approx \mathrm{e}^{j\Delta x\sqrt{k^2-k_y^2}}\mathrm{e}^{j\Delta x\sqrt{k^2-k_z^2}}\mathrm{e}^{-jk\Delta x} = K_1(k_y)K_2(k_z)k_0 \quad (2)$$

where $K_1(k_y)$ and $K_2(k_z)$ are the expansion terms of the diffraction factors

$$\begin{aligned} K_1(k_y) &= \mathrm{e}^{j\Delta x\sqrt{k^2-k_y^2}} \\ K_2(k_z) &= \mathrm{e}^{j\Delta x\sqrt{k^2-k_z^2}}. \end{aligned} \quad (3)$$

More specifically, the step calculation can be realized by alternating the two directions of the row and column, as depicted in Fig. 2. As a result, the calculation resources can be largely saved.

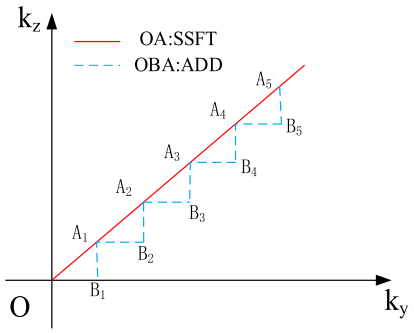

Fig. 2. Iterative process of the traditional SSFT algorithm is carried out along the red solid line, that is $O \rightarrow A_i$, while the iterative step of the alternating direction decomposition is carried out along the blue dotted line, i.e., $O \rightarrow B_i \rightarrow A_i$.

A 3-D scalar PE in terms of the ADD-SSFT is given by

$$\begin{aligned} u\left(x+\Delta x, y, z\right) = &\sqrt{k_0\eta\left(x+\Delta x\right)} \\ &\times T_2\left[\sqrt{k_0\eta\left(x+\Delta x/2\right)}T_1\left(u\right)\right] \end{aligned} \quad (4)$$

where $k_0 = \mathrm{e}^{-jk\Delta x}$, k is the free space wavenumber, $n = 1$ is the air refractive index, and $\eta = \mathrm{e}^{jk\Delta x(n-1)}$ donates the refraction term in PE calculation. Moreover, T_1 represents the local one-dimensional stepping process along the y direction, T_2 is the local one-dimensional stepping process along the z direction, and they can be given by

$$\begin{aligned} T_1\left(u\right) &= \frac{1}{2\pi}\int\left[K_1\left(k_y\right)\int u(y, z)\mathrm{e}^{-jk_y y}d_y\right]\mathrm{e}^{jk_y y}dk_y \\ T_2\left(u\right) &= \frac{1}{2\pi}\int\left[K_2\left(k_z\right)\int u(y, z)\mathrm{e}^{-jk_z z}d_z\right]\mathrm{e}^{jk_z z}dk_z. \end{aligned} \quad (5)$$

The first type of boundary condition (Dirichlet boundary condition) is used at the boundary of the obstacle, which can be given by

$$u\left(x, y, z\right) = 0. \quad (6)$$

The electric field of each point-source receiving antenna on the receiving surface can be obtained by

$$u_{mn} = u\left(y_i, z_j\right) \quad (7)$$

with

$$\begin{aligned} y_i &= y0 + (i-1)\left\lceil N_y/\left(\mathrm{N}-1\right)\right\rceil \\ z_j &= z0 + (j-1)\left\lceil N_z/\left(\mathrm{N}-1\right)\right\rceil \end{aligned} \quad (8)$$

where m is the number of antennas on the receiving plane, ranging from 1 to N_R, n is the number of antennas on the transmitting surface, ranging from 1 to N_T, (y_0, z_0) is the position of the first point-source on the front, i and j are the numbers of point-sources along the y or z directions respectively, and they can be set as 1 to N.

The sum of the fields radiating from all the point sources on the transmitting plane gets the receiving field at a single point source on the receiving surface, i.e.,

$$g_m = \sum_{n=1}^{N_T} u_{mn}. \quad (9)$$

Therefore, the channel matrix $\mathbf{H}$ of the EM channel model can be derived as

$$\mathbf{H} = \begin{bmatrix} u_{11} & u_{12} & \cdots & u_{1N_T} \\ u_{21} & u_{22} & \cdots & u_{2N_T} \\ \vdots & \vdots & \ddots & \vdots \\ u_{N_R1} & u_{N_R2} & \cdots & u_{N_RN_T} \end{bmatrix}. \tag{10}$$

B. Vector EM Channel Model Based on the ADD-SSFT PE Method

Due to the particularity of the point source, in order to model the communication channel with full polarizations, dyadic Green's function is used to calculate the polarization of the field. The dyadic Green's function in free space is

$$\overline{G}\left(r, r'\right) = \left(\bar{I} + \frac{\nabla\nabla}{k_0^2}\right) g_0\left(r, r'\right) \tag{11}$$

where $\bar{\mathbf{I}}$ is the unit dyadic tensor, The matrix representation of $\bar{\mathbf{G}}$ is

$$\bar{\mathbf{G}} = \begin{bmatrix} G_{xx} & G_{xy} & G_{xz} \\ G_{yx} & G_{yy} & G_{yz} \\ G_{zx} & G_{zy} & G_{zz} \end{bmatrix} \tag{12}$$

where each element is a scalar Green's function and the subscript represents the correspondence between a polarization of the field and a polarization of the source.

For the convenience of analysis, the obstacles are assumed to be perfect electric conductors and the corresponding boundary condition is given by

$$\mathbf{e}_n \times \mathbf{E} = 0 \tag{13}$$

where $\mathbf{e}_n$is the normal direction and $u = \mathbf{E}\mathrm{e}^{-jkx}$.

As we know, the vector PE is formed by the union of three scalar PEs. However, due to the specificity of the point source, the EM field components of the three PEs cannot be determined, and the polarization field excited at the obstacle cannot also be obtained directly. Nevertheless, the polarization fields on each PEC face of the obstacle can be obtained with Dyadic Green's function. Similar to the scalar case, according to the boundary conditions (13), for the first face along the axial direction (x-axis), the presence of only an x-polarized electric field can be determined. Suppose that a set of point sources on the source plane are excited with the complex amplitudes t_{zn} along the z-polarized, then the x-polarized electric field g_m^x that is generated in the first face of the axial direction would be

$$g_m^x = \sum_{n=1}^{N_T} G_{xz}\, t_{zn} = \sum_{n=1}^{N_T} u_{mn}^{xz}. \tag{14}$$

Similarly, the fields excited by the complex amplitude along the z-polarized can be obtained on all faces of the whole obstacle. Afterward, the excited field is brought into the PE as a source at the obstacle for iteration to the receivers. Therefore, based on the x-polarized electric field generated by point sources which are excited with the complex polarization along z-polarized, the channel matrix of the EM channel model can be obtained as

$$H_{xz} = \begin{bmatrix} u_{11}^{xz} & u_{12}^{xz} & \cdots & u_{1N_T}^{xz} \\ u_{21}^{xz} & u_{22}^{xz} & \cdots & u_{2N_T}^{xz} \\ \vdots & \vdots & \ddots & \vdots \\ u_{N_R1}^{xz} & u_{N_R2}^{xz} & \cdots & u_{N_RN_T}^{xz} \end{bmatrix}. \tag{15}$$

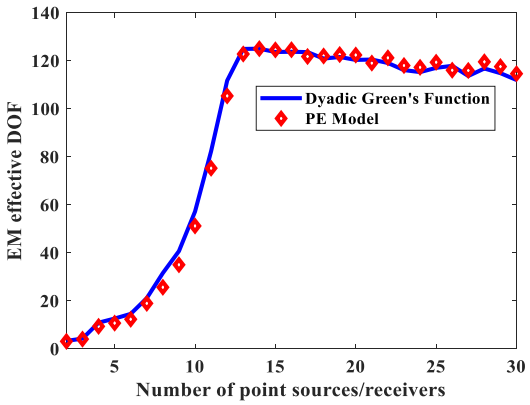

Fig. 3. Comparison between the EM effective DOFs calculated with the proposed PE Model and the dyadic Green's function.

Referring to the scalar channel matrix described in Section II-A, the channel matrix can be obtained from the above process. The vector channel matrix can be understood as the combination of nine scalar channel matrices.

Therefore, the vector channel matrix can be deduced as

$$H = \begin{bmatrix} H_{xx} & H_{xy} & H_{xz} \\ H_{yx} & H_{yy} & H_{yz} \\ H_{zx} & H_{zy} & H_{zz} \end{bmatrix}. \tag{16}$$

C. EM EDOF

In MIMO wireless communications, the EM DOF refers to the number of significant EM modes/eigenvalues, which is frequently used for characterizing the performance of spatial multiplexing brought by MIMO technology [35], [3], [36], [37]. But it would be tedious to count the significant EM modes for each configuration, therefore, EDOF is used here for the convenience of analyses.

The one-sample Pearson correlation matrix [38] of the EM channel model is

$$\mathbf{R_r} = \mathcal{N}\left[\mathbf{H}\mathbf{H}^{\dagger}\right] \tag{17}$$

where $\mathcal{N}$ represents the normalization, $\mathbf{H}$ is the channel matrix of the EM channel model, and † is the Hermitian operator.

Therefore, the EDOF can be calculated by [37]

$$\psi_e\left(\mathbf{R_r}\right) = \left(\frac{tr\left(\mathbf{R_r}\right)}{\|\mathbf{R_r}\|_F}\right)^2 = \frac{\left(\sum_i \sigma_i\right)^2}{\sum_i \sigma_i^2} \tag{18}$$

where F denotes the Frobenius norm, $tr\left(\cdot\right)$ represents the trace operator, and $\sigma_i$is the ith eigenvalue of $\mathbf{R_r}$.

The eigenvalue of this correlation matrix is expressed as the intensity of the independent EM modes. If the eigenvalue is larger, the effect on communication or information transmission is greater. As shown in Fig. 3, the EM channel model based on the ADD-SSFT PE method is used to verify the EDOF limit in the free space, which is compared with the free space analytical solution based on Dyadic Green's function. It can be seen that when the EM EDOF reaches the limit, the corresponding limit values of both the proposed ADD-SSFT PE method and the analytic solution are consistent, which validates the proposed method.

III. Numerical Results

A. PE Model Accuracy Verification

At first, the accuracy of the proposed PE Model can be verified by comparing the electric field distribution with the method of moment

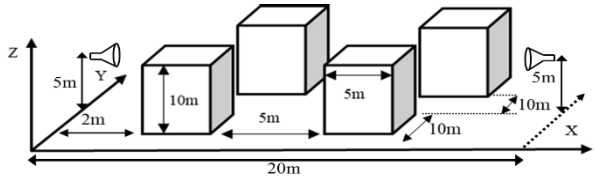

Fig. 4. Model of propagation with obstacles.

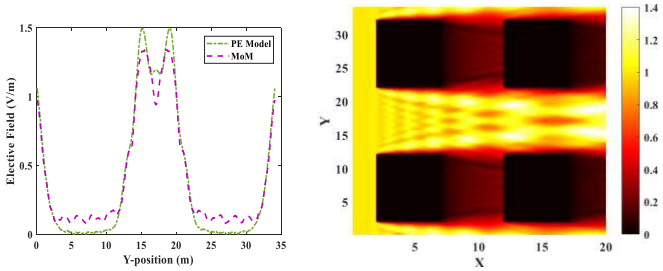

Fig. 5. (a) Comparison of field values between the PE Model and MoM at $z = 5$ m. (b) Electric field propagation diagram.

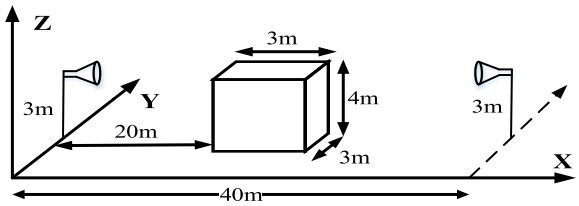

Fig. 6. Single cube obstacle model.

(MoM). A simplified model composed of four cubic obstacles is analyzed at the frequency of 300 MHz and the distribution map is given in Fig. 4. The comparison of the electric field distribution is made between the MoM (benchmark) and the proposed PE Model.

B. Influence of Different Polarizations on Channel EM EDOF

The influence of different polarizations on EM EDOF is analyzed; the model is shown in Fig. 6. As depicted in Fig. 7(a), in a communication channel with full vectorial EM fields, the copolarization (*XX*, *YY*, *ZZ*) EM wave plays a major role in the EDOF.

It should be noted that the valid polarization of current sources may be radically different in the near-field or far-field. In the case of the side length with $L = 5\lambda_0$, the number of antennas is fixed at 11×11. The antennas here refer to the isotropic point sources. And the reactive near-field, radiative near-field, and far-field can be calculated as $D \leq 0.62(L^3/\lambda)^{1/2}$, $0.62(L^3/\lambda)^{1/2} \leq D \leq 2L^2/\lambda$, $2L^2/\lambda \leq D$, respectively. At the reactive near-field, the EDOF calculated by full polarizations consisting of three polarizations of the current source (X, Y, Z directions) is higher than that by two horizontal polarizations (Y, Z directions). However, at the radiative near-field and far-field, the EDOF is the same for both cases, which is clearly illustrated in Fig. 7(b). This fully demonstrates that the contribution of near-field communication for the x polarization only appears in the relatively near-field. The contribution of x polarization disappears when the distance exceeds the near-field scope.

C. Influence of Obstacle With Different Heights on the Communication Performance

Since the obstacles exist in half-space, the transmitted EM signals will be blocked, reflected, and diffracted by the peak obstacle. The channel capacity of the communication will definitely be affected. A representative channel model is shown in Fig. 8. The region

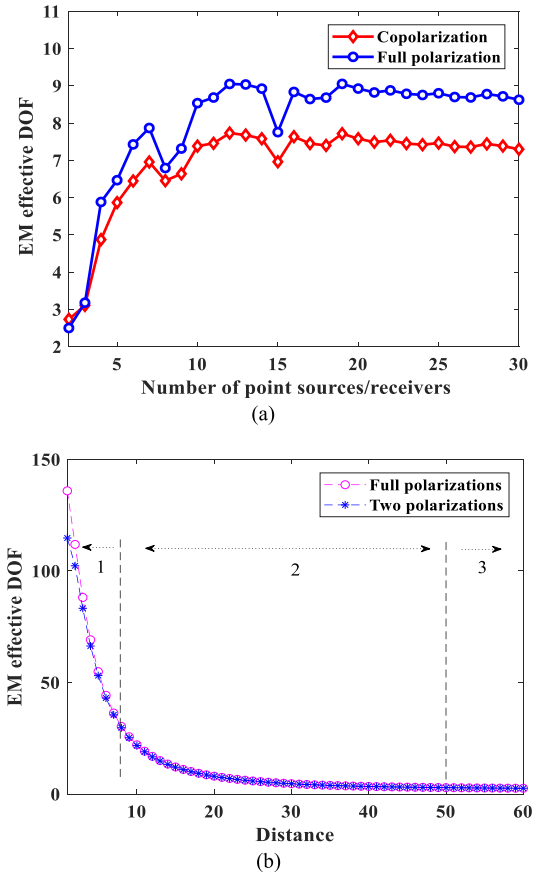

Fig. 7. (a) Comparison of EM effective DOF between full polarizations and copolarizations in free space. (b) EM EDOFs calculated with different polarizations, 1: reactive near-field; 2: radiative near-field; 3: far-field, the side length $L = 5\lambda_0$, antenna number $N = 11$ and distance $D = 1 - 13\lambda_0$.

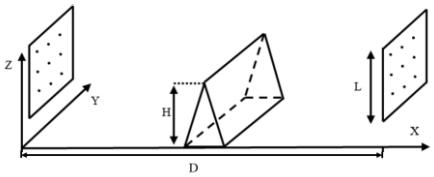

Fig. 8. Communication model of a single peak environment. The region between the transmitting and receiving planes (with dots) all fall into the near-field region.

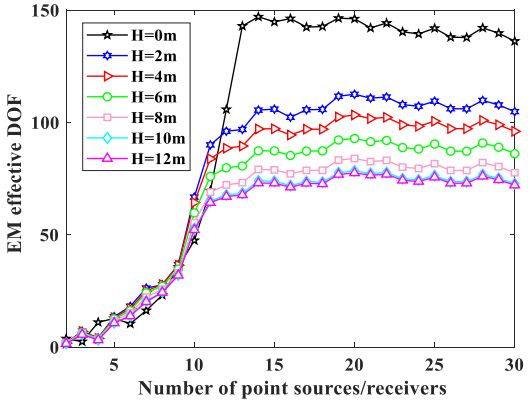

Fig. 9. Comparison of EDOFs for different peak heights at near-field. The source/receiving plane size is $10 \times 10\lambda$, $D = 8$ m.

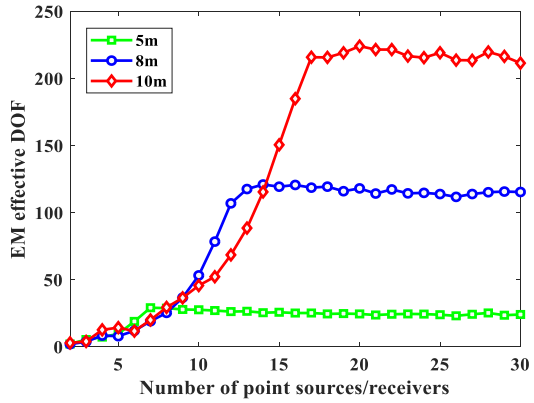

Fig. 10. Influences of different antenna array sizes and antenna numbers on the EM EDOF.

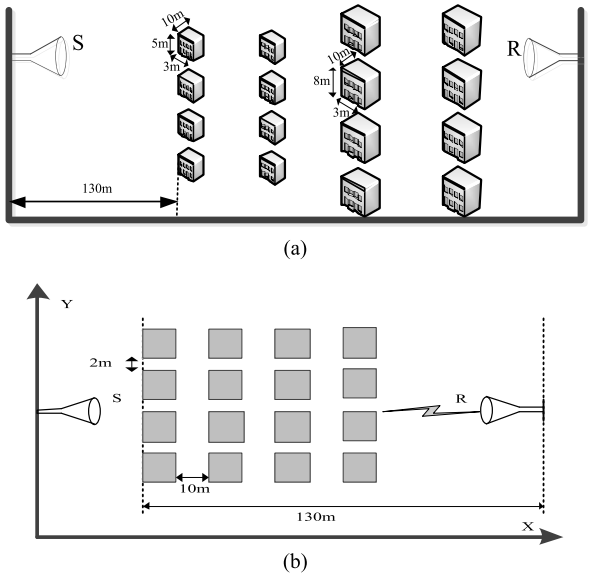

Fig. 11. (a) Channel model in urban residential building environment and (b) Top view of the channel model.

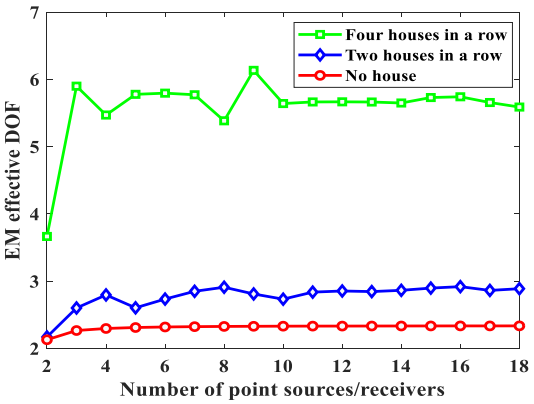

Fig. 12. Comparisons of EDOF limit with and without houses at far-field.

between the transmitting and receiving planes all fall into the near-field region. As shown in Fig. 9, the influence of a large single peak with different heights on the communication performance is analyzed. The EM EDOFs with a single peak are reduced as a whole when compared with the free space scenario. Moreover, the EM EDOF is reduced with the increase of the peak height. The EM EDOF becomes saturated when the peak height is larger than the height of the receiving/transmitting plane.

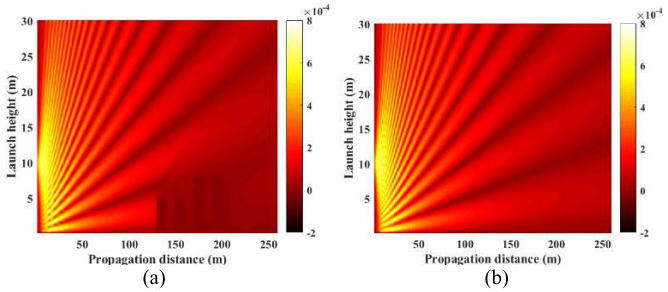

Fig. 13. Distribution diagrams of the electric fields for the urban model (a) with houses and (b) without houses.

D. Influence of Antenna Array Size on Communication Performance

From the viewpoint of EM information theory, the limit of EDOF is related to the size of the transmitting plane. When the size of the transmitting surface is fixed, the limit of EM EDOF of the channel is determined by its surrounding environments. It should be noted that the number of receivers is equal to the number of point sources. As shown in Fig. 10, the influence of antenna array size on the channel EDOF in the single-peak communication environment is analyzed. It can be seen that with the increasing antenna array size, the limit of EDOF changes. But as the number of antennas increases, the EDOF cannot be increased further when reaching a saturated value.

E. Impact of Urban Housing on Communication Performance

In the finite space communication system, the system has the best performance when the number of transmitting and receiving antennas reaches the saturation point, and the EM effective DOF reaches the limit. However, in the actual urban environment, the ground and buildings have a great influence on the propagation of EM waves, and the performance of the communication system will be greatly affected. An urban model is established in Fig. 11. The $10 \times 10\lambda$ point-source array antenna is used for transmitting, and the lowest height of the transmitting and receiving array is located at 5 m.

As shown in Fig. 12, the EM EDOF is analyzed for this urban model with and without the houses. In the near-field, these houses may block the propagation of the EM waves. While in the far-field, the multipath effect caused by building diffraction and ground reflection leads to increased EDOF. And with the increase in the number of houses, the propagation of radio waves is not in a single direction, resulting in the increase of EDOF. Additionally, the distribution diagrams of the electric fields are given in Fig. 13.

IV. Conclusion

The EM channel model based on the ADD-SSFT PE method is established. The proposed PE Model is verified by comparing it with the free space analytical solution. The main influence of copolarization on communication performance is discussed. By comparing the free space to the half-space (PEC ground) and the obstacle in the half-space, the influences of the ground and obstacle on the EDOF are calculated and analyzed in detail. At the far-field, the presence of ground and obstacles leads to multiple scattering and multipath effects, which have increased the EDOF. But in the near-field, the EDOFs decrease by the obstacles. It is worth noting that the EDOF increases with the increased sizes of the transmitting and receiving planes, but as the number of antennas increases, the EDOF cannot be further increased when reaching a saturated value.

REFERENCES

[1] C. E. Shannon, "A mathematical theory of communication," *Bell Syst. Tech. J.*, vol. 27, no. 3, pp. 379–423, 1948.

[2] E. G. Larsson, O. Edfors, F. Tufvesson, and T. L. Marzetta, "Massive MIMO for next generation wireless systems," *IEEE Commun. Mag.*, vol. 52, no. 2, pp. 186–195, Feb. 2014.

[3] T. Muharemovic, A. Sabharwal, and B. Aazhang, "Antenna packing in low-power systems: Communication limits and array design," *IEEE Trans. Inf. Theory*, vol. 54, no. 1, pp. 429–440, Jan. 2008.

[4] D. Tse and P. Viswanath, *Fundamentals of Wireless Communication*. Cambridge, U.K.: Cambridge Univ. Press, 2005.

[5] S. S. A. Yuan, Z. He, X. Chen, C. Huang, and W. E. I. Sha, "Electromagnetic effective degree of freedom of an MIMO system in free space," *IEEE Antennas Wireless Propag. Lett.*, vol. 21, no. 3, pp. 446–450, Mar. 2022.

[6] A. A. Zaporozhets and M. F. Levy, "Bistatic RCS calculations with the vector parabolic equation method," *IEEE Trans. Antennas Propag.*, vol. 47, no. 11, pp. 1688–1696, Nov. 1999.

[7] M. F. Levy and P. P. Borsboom, "Radar cross-section computations using the parabolic equation method," *Electron. Lett.*, vol. 32, no. 13, pp. 1234–1236, Jun. 1996.

[8] Z. He, Z. H. Fan, D. Z. Ding, and R. S. Chen, "A vector parabolic equation method combined with MLFMM for scattering from a cavity," *Appl. Comput. Electromagn. Soc. J.*, vol. 30, no. 5, pp. 496–502, 2015.

[9] Z. He, T. Su, and R. S. Chen, "Vector parabolic equation method for the EM scattering from PEC objects in half-space," *Appl. Comput. Electromagn. Soc. J.*, vol. 30, no. 8, pp. 877–883, 2015.

[10] R. Martelly and R. Janaswamy, "Modeling radio transmission loss in curved, branched and rough-walled tunnels with the ADI-PE method," *IEEE Trans. Antennas Propag.*, vol. 58, no. 6, pp. 2037–2045, Jun. 2010.

[11] S. Mckee, D. P. Wall, and S. K. Wilson, "An alternating direction implicit scheme for parabolic equations with mixed derivative and convective terms," *J. Comput. Phys.*, vol. 126, no. 1, pp. 64–76, 1996.

[12] C. A. Zelley and C. C. Constantinou, "A three-dimensional parabolic equation applied to VHF/UHF propagation over irregular terrain," *IEEE Trans. Antennas Propag.*, vol. 47, no. 10, pp. 1586–1596, Oct. 1999.

[13] Z. He and R. S. Chen, "A vector meshless parabolic equation method for three-dimensional electromagnetic scatterings," *IEEE Trans. Antennas Propag.*, vol. 63, no. 6, pp. 2595–2603, Jun. 2015.

[14] Z. He and R. S. Chen, "A novel parallel parabolic equation method for electromagnetic scatterings," *IEEE Trans. Antennas Propag.*, vol. 64, no. 11, pp. 4777–4784, Nov. 2016.

[15] Z. He, H. Zeng, and R. S. Chen, "Two-way propagation modeling of expressway with vehicles by using the 3-D ADI-PE method," *IEEE Trans. Antennas Propag.*, vol. 66, no. 4, pp. 2156–2160, Apr. 2018.

[16] Q. Guo, C. Zhou, and Y. Long, "Greene approximation wide-angle parabolic equation for radio propagation," *IEEE Trans. Antennas Propag.*, vol. 65, no. 11, pp. 6048–6056, Nov. 2017.

[17] M. F. Levy, "Parabolic equation modelling of propagation over irregular terrain," *Electron. Lett.*, vol. 26, no. 15, pp. 1153–1155, Jul. 1990.

[18] R. J. McArthur, "Propagation modelling over irregular terrain using the split-step parabolic equation method," in *Proc. Radar*, vol. 92. Oct. 1992, pp. 54–57.

[19] L. Zhou, D. Wang, Z. Mu, X. Xi, and L. He, "LF radio wave prediction at short ranges with high propagation angles over irregular terrain," *IEEE Antennas Wireless Propag. Lett.*, vol. 16, pp. 732–735, 2017.

[20] D.-D. Wang, X.-L. Xi, Y.-R. Pu, J.-S. Zhang, and L.-L. Zhou, "LF groundwave propagation modeling over irregular terrain by the hybrid two-way parabolic equation method," *IEEE Trans. Antennas Propag.*, vol. 67, no. 10, pp. 6596–6601, Oct. 2019.

[21] Z. He, T. Su, H.-C. Yin, and R.-S. Chen, "Wave propagation modeling of tunnels in complex meteorological environments with parabolic equation," *IEEE Trans. Antennas Propag.*, vol. 66, no. 12, pp. 6629–6634, Dec. 2018.

[22] H. Qin and X. Zhang, "Efficient modeling of radio wave propagation in tunnels for 5G and beyond using a split-step parabolic equation method," in *Proc. 34th Gen. Assem. Sci. Symp. Int. Union Radio Sci. (URSI GASS)*, Aug. 2021, pp. 1–3.

[23] Y. S. Li, Y. Q. Bian, Z. He, and R.-S. Chen, "EM pulse propagation modeling for tunnels by three-dimensional ADI-TDPE method," *IEEE Access*, vol. 8, pp. 85027–85037, 2020.

[24] X. Zhang and C. D. Sarris, "Statistical modeling of electromagnetic wave propagation in tunnels with rough walls using the vector parabolic equation method," *IEEE Trans. Antennas Propag.*, vol. 67, no. 4, pp. 2645–2654, Apr. 2019.

[25] M. S. Lytaev, "Numerov-Padé scheme for the one-way Helmholtz equation in tropospheric radio-wave propagation," *IEEE Antennas Wireless Propag. Lett.*, vol. 19, no. 12, pp. 2167–2171, Dec. 2020.

[26] Q. Guo and Y. Long, "Two-way parabolic equation method for radio propagation over rough sea surface," *IEEE Trans. Antennas Propag.*, vol. 68, no. 6, pp. 4839–4847, Jun. 2020.

[27] J. Ramakrishna, "Path loss predictions in the presence of buildings on flat terrain: A 3-D vector parabolic equation approach," *IEEE Trans. Antennas Propag.*, vol. 51, no. 8, pp. 1716–1728, Aug. 2003.

[28] R. Janaswamy and J. B. Andersen, "Path loss predictions in urban areas with irregular terrain topography," *Wireless Pers. Commun.*, vol. 12, no. 3, pp. 255–268, 2000.

[29] G. L. Ramos et al., "Parabolic equation technique applied to an urban scenario in Rio De Janeiro," in *Proc. Telecoms Conf. (ConfTELE)*, Feb. 2021, pp. 1–4.

[30] L. Zhou, C. Liao, X. Xiong, Q. Zhang, and D. Zhang, "An alternative direction decomposition scheme and error analysis for parabolic equation model," *IEEE Trans. Antennas Propag.*, vol. 65, no. 5, pp. 2547–2557, May 2017.

[31] D. A. B. Miller, "Waves, modes, communications, and optics: A tutorial," *Adv. Opt. Photon.*, vol. 11, no. 3, pp. 679–825, 2019.

[32] X. Chen et al., "Revisit to mutual coupling effects on multi-antenna systems," *J. Commun. Inf. Netw.*, vol. 5, no. 4, pp. 411–422, Dec. 2020.

[33] R. Piestun and D. A. B. Miller, "Electromagnetic degrees of freedom of an optical system," *J. Opt. Soc. Amer. A, Opt. Image Sci.*, vol. 17, no. 5, pp. 892–902, 2000.

[34] X. Chen, S. Zhang, and Q. Li, "A review of mutual coupling in MIMO systems," *IEEE Access*, vol. 6, pp. 24706–24719, 2018.

[35] D.-S. Shiu, G. J. Foschini, M. J. Gans, and J. M. Kahn, "Fading correlation and its effect on the capacity of multielement antenna systems," *IEEE Trans. Commun.*, vol. 48, no. 3, pp. 502–513, Mar. 2000.

[36] S. Verdu, "Spectral efficiency in the wideband regime," *IEEE Trans. Inf. Theory*, vol. 48, no. 6, pp. 1319–1343, Jun. 2006.

[37] Y. Wang et al., "Improvement of diversity and capacity of MIMO system using scatterer array," *IEEE Trans. Antennas Propag.*, vol. 70, no. 1, pp. 789–794, Jan. 2022.

[38] G. Grimmett and D. Stirzaker, *Probability and Random Processes*, 3rd ed. Oxford, U.K.: Oxford Univ. Press, 2001.